LBL-38609
UC-406

# ERNEST ORLANDO LAWRENCE BERKELEY NATIONAL LABORATORY

# Electrode Design for Coplanar-Grid Detectors

P.N. Luke, M. Amman, T.H. Prettyman,
P.A. Russo, and D.A. Close
**Engineering Division**

November 1996
Presented at the
*1996 IEEE Nuclear Science Symposium*,
Los Angeles, CA,
November 12–15, 1996,
and to be published in
the Proceedings

REFERENCE COPY
Does Not
Circulate
Bldg. 50 Library.
LBL-38609
Copy 1

## DISCLAIMER

This document was prepared as an account of work sponsored by the United States Government. While this document is believed to contain correct information, neither the United States Government nor any agency thereof, nor the Regents of the University of California, nor any of their employees, makes any warranty, express or implied, or assumes any legal responsibility for the accuracy, completeness, or usefulness of any information, apparatus, product, or process disclosed, or represents that its use would not infringe privately owned rights. Reference herein to any specific commercial product, process, or service by its trade name, trademark, manufacturer, or otherwise, does not necessarily constitute or imply its endorsement, recommendation, or favoring by the United States Government or any agency thereof, or the Regents of the University of California. The views and opinions of authors expressed herein do not necessarily state or reflect those of the United States Government or any agency thereof or the Regents of the University of California.

LBL-38609
UC-406

# Electrode Design for Coplanar-Grid Detectors

P.N. Luke,[1] M. Amman,[1] T.H. Prettyman,[2] P.A. Russo,[2] and D.A. Close[2]

[1]Engineering Division
Ernest Orlando Lawrence Berkeley National Laboratory
University of California
Berkeley, California 94720

[2]Los Alamos National Laboratory
Los Alamos, New Mexico 87545

November 1996

This work was supported at LBNL by the U.S. Department of Defense, Office of Special Technology, Technical Support Working Group Project Number T-135 through the U.S. Department of Energy under Contract No. DE-AC03-76SF00098. The detector modeling effort is supported at LANL by the U.S. Department of Energy, Office of Nonproliferation and National Security.

# Electrode Design for Coplanar-Grid Detectors

P. N. Luke[1], M. Amman[1], T. H. Prettyman[2], P. A. Russo[2], and D. A. Close[2]
[1]Ernest Orlando Lawrence Berkeley National Laboratory, Berkeley, California 94720
[2]Los Alamos National Laboratory, Los Alamos, New Mexico 87545

*Abstract*

The coplanar-grid charge sensing technique provides a method for improving the spectral response of gamma-ray detectors based on compound semiconductors, which typically have poor charge transport properties. The technique functions by effectively modifying the charge induction characteristics of the detector such that the dependence of detector signal on the depth of radiation interaction is minimized. The effectiveness of this technique however can be compromised by non-uniform charge induction characteristics across the detector. This paper examines such non-uniformity due to fringe effects near the detector edges. Alternate electrode configurations are studied that provide effective compensation for such effects. Results from experimental measurements and computer simulations are presented.

## I. INTRODUCTION

High atomic-number, wide bandgap semiconductors are potential candidates for use as room temperature gamma-ray detectors. Based on charge generation statistics considerations, it is in principle possible for these detectors to achieve energy resolution within a small factor of that of liquid-nitrogen cooled Ge detectors. Among the semiconductors investigated for this application, $HgI_2$ and CdTe have undergone extensive development [1]. CdZnTe is a more recently developed material that possesses significant advantages over the earlier materials [2]. All of these compound semiconductors however have poor charge transport properties, with mobility-lifetime products for electrons and holes that are 100 to 1000 times lower than that of Ge. This generally results in poor energy resolution when conventional detector structures and electronics are used. Recently, the coplanar-grid charge sensing technique was introduced as a method to deal with such charge transport deficiencies so that substantially improved spectral performance can be obtained [3]. Estimates based on a highly simplified model have shown that energy resolution close to the statistical limit may be possible, even with the currently achieved mobility-lifetime products for some of these materials [4]. This model, however, did not consider the many effects that can degrade detector performance, such as material non-uniformity, edge effects, Compton scattering, electronic noise and charge trapping statistics. Some of the effects of material non-uniformity have been investigated previously [4]. In this paper, we will consider detector design issues. In particular, edge effects and electrode designs for compensating such effects are addressed. Experimental results from detectors with different electrode configurations will be presented and compared to calculations obtained using a computer model recently developed to simulate the response of room temperature semiconductor detectors [5], [6].

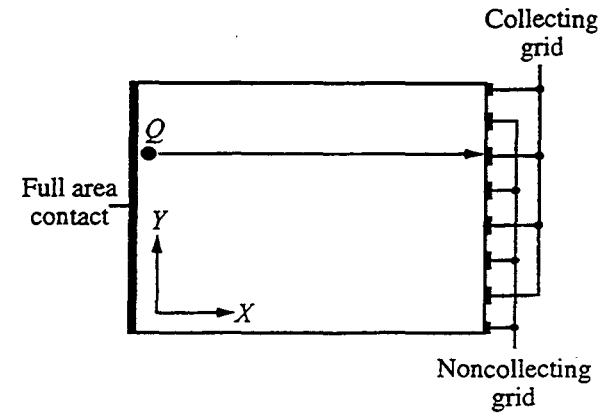


Figure 1. Simple coplanar-grid structure.

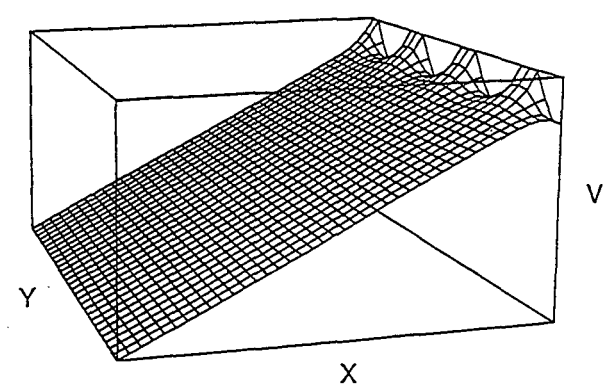


Figure 2. Calculated potential distribution for the simple coplanar-grid detector of Fig. 1 under typical operating bias conditions. The bias between the grids is a tenth that across the detector. The calculation was done neglecting effects caused by the detector boundaries.

## II. THE COPLANAR-GRID TECHNIQUE AND EDGE EFFECTS

In a coplanar-grid detector, two electrodes are used to sense the collection of charge carriers. A typical electrode configuration consists of a set of linear strip electrodes, which are interconnected to form two independent, interdigitated grid electrodes (Fig. 1). Under operation, a bias voltage is applied across the detector to collect the carriers, with the electrons being collected towards the grid electrodes. An additional bias voltage is applied between the two grid electrodes such that all the electrons are collected at only one of the grid electrodes (collecting grid). This voltage is small compared to the bias voltage applied across the detector so that the electric field inside the detector remains substantially uniform (Fig. 2).

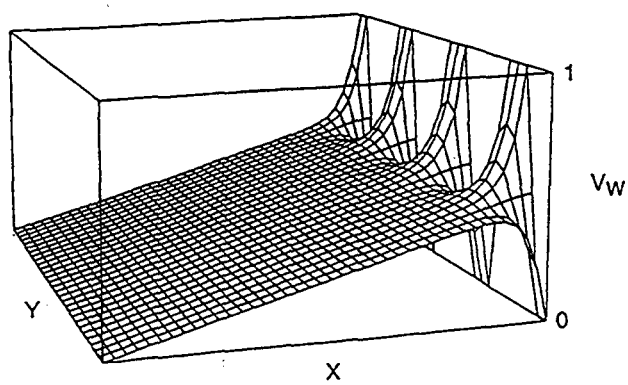


Figure 3. Calculated collecting grid weighting potential distribution for the simple coplanar-grid detector of Fig. 1. The calculation was done neglecting effects caused by the detector boundaries.

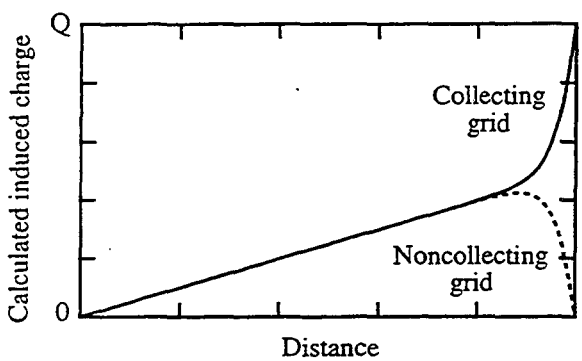


Figure 4. Calculated induced charge on the grid electrodes of the simple coplanar-grid detector of Fig. 1 as a function of the distance traveled by a charge $Q$ originating near the full area contact and ultimately collected on the collecting grid electrode. Effects due to charge trapping are ignored.

The characteristics of the induced signal on a grid electrode as a result of charge movement can be determined using the weighting potential method [7]. The weighting potential, $V_w$, for a specific electrode is calculated with the conditions that the electrode is at unit potential, all other electrodes are at zero potential, and no space charge exists. The incremental induced charge on the electrode due to the movement of a charge $Q$ is then given by

$$\Delta Q_{ind} = Q\,\Delta V_w \qquad (1)$$

where $\Delta V_w$ is the change in $V_w$ over the path traversed by the charge $Q$. The weighting potential distribution for a grid electrode in an idealized coplanar-grid device is shown in Fig. 3. The weighting potential distribution for the other grid electrode is identical except that it is displaced in the $Y$ direction by one strip pitch. The induced signals on these electrodes can then be obtained by simply projecting the path of a moving charge onto their respective weighting potential distributions. Figure 4 shows the shape of the signals due to a charge $Q$ moving from the cathode to the collecting grid as illustrated in Fig. 1. By subtracting the two signals, a net signal is obtained, which can be varied depending on the

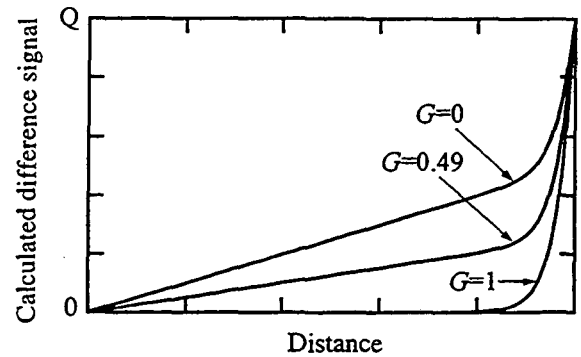


Figure 5. Calculated differential induced charge signal between the grid electrodes of the simple coplanar-grid detector of Fig. 1 as a function of the distance traveled by a charge $Q$. The plots are for various values of $G$ which is the fraction of the noncollecting grid induced charge subtracted from the collecting grid induced charge. Effects due to charge trapping are ignored.

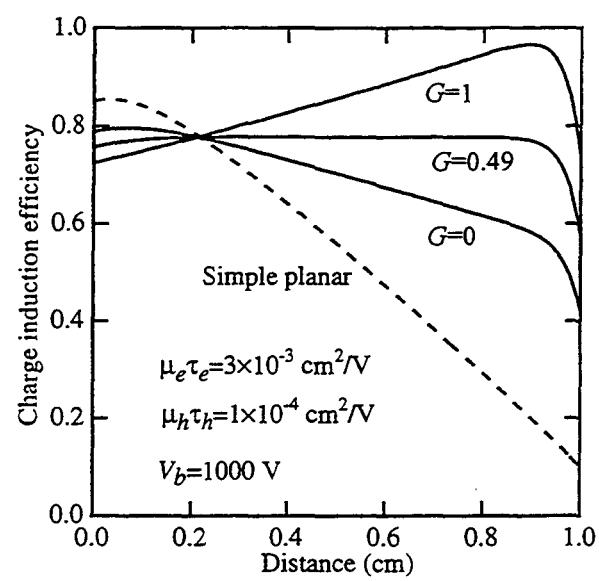


Figure 6. Calculated charge induction efficiency as function of distance from the full area contact for the simple coplanar-grid detector of Fig. 1. The bias applied across the detector is $V_b$. For this detector the optimal value of $G$ is 0.49. The charge induction efficiency for a simple planar detector is highly non-uniform and is shown for comparison purposes.

relative gain ($G$) of the two signals (Fig. 5). Adjusting the relative gain therefore effectively changes the charge induction characteristics of the detector. This allows the detector response to be optimized according to the material's carrier transport properties to provide the best energy resolution. A way to show the improvement in detector response is to plot the charge induction efficiency, which is the net induced charge normalized to the charge initially created, as a function of the position where the charge is originally created. Figure 6 shows such a plot for a 1 cm thick detector with different values of $G$. In this example, $G = 0.49$ gives the most uniform response and thus the best energy resolution. The charge transport parameters used in this calculation are within the typical range of values found in CdZnTe crystals. In comparison, a detector

with the simple planar geometry displays a strongly varying response, as shown by the dashed line in Fig. 6. Such variation is the main reason for the very poor energy resolution commonly observed in planar detectors.

The simple analysis above ignored the effects of boundaries that necessarily exist for a real detector. A realistic calculation of the weighting potential must take into account the effects of fringing field near the edge of the detector. Such edge effects can produce significant distortion in the weighting potential, resulting in non-uniform charge induction characteristics, which in turn can degrade energy resolution. To investigate edge effects, we have carried out experimental measurements and computer simulations.

## III. METHODS

Experiments were performed using a CdZnTe crystal with an area of $9.6 \times 9.6$ mm$^2$ and a thickness of 8.5 mm. Three different coplanar-grid electrode structures were examined. The same CdZnTe crystal has been used in each case to avoid confusion due to material differences. The charge induction characteristics of the detector were measured using a collimated alpha particle source ($^{241}$Am) in a vacuum chamber. Translation stages inside the chamber allow the detector to be scanned in situ. Gamma-ray spectral response was obtained with a $^{137}$Cs source.

Simulations of detector response were made using a recently developed computer model. A detailed description of the computational methods and experimental validations is provided elsewhere [5], however the general approach is outlined here. In the model, both the production and collection of charge carriers are treated. A three-dimensional Monte Carlo simulation is used to model the production of charge carriers by gamma-ray interactions, which include Compton and photoelectric interactions. Charge carrier drift and induction are modeled in a separate calculation. This involves the use of finite element analysis to compute the electric field in the detector and the weighting potential for the electrodes. Currently, a two-dimensional model is used for this calculation. From the electric field, the trajectory of the electrons and holes are determined. The trapping of charge carriers is modeled in the calculation. Once the trajectory of the carriers and their population are known, the induced signal at an electrode can be calculated using the weighting potential. From this calculation, a two-dimensional charge induction efficiency map is generated. The induction efficiency map is then used in the Monte Carlo calculation to determine the induced charge signal for each gamma-ray interaction. For the coplanar-grid detectors, a charge induction map is generated for each grid electrode. The two charge induction maps are subtracted, with the relative gain ($G$) as an adjustable parameter, to produce a single induction map. This simulates the response of the signal subtraction circuit. Noise associated with charge carrier production, trapping, and electronic noise can be included in the calculation. In this work, we assumed that the material properties are spatially uniform. The electron and hole mobility-lifetime products used in the calculation were $4.8\times10^{-3}$ cm$^2$/V and $2.5\times10^{-4}$ cm$^2$/V, respectively, which are approximately the measured values for the CdZnTe crystal used in the experiment.

## IV. RESULTS

### A. Simple Grid Pattern

Figure 7 shows the electrode pattern used for a simple coplanar-grid structure. It consists of a series of linear strip electrodes of equal width and gap. For this detector structure, the calculated equipotential contour plot of the weighting potential for the collecting grid electrode is shown in Fig. 8. Non-uniformity in the weighting potential within the bulk of the detector is evident from the increasing tilt of the contour lines in moving from the full contact surface to the gridded surface. The weighting potential for the noncollecting grid electrode is a mirror image of this potential and hence varies in the opposite sense. The characteristics of the induced charge at the grid electrodes resulting from drifting charge within the detector are also non-uniform across the detector since they are determined from the weighting potentials. The calculated induced charge signals from the two grid electrodes for charge drifting from the full contact surface to the gridded surface are shown in Fig. 9 for the three positions indicated. The poor uniformity in charge induction is evidenced by the significant differences between the two grid signals taken near the edges. Selecting a certain value of $G$ for optimal charge induction for charge originating near the middle of the detector will give non-optimal induction for events away from the center, leading to a degradation in the detector resolution. The actual induced signals from the detector were observed by scanning a collimated alpha particle source across the full-area contact. Figure 10 shows the captured waveforms at the three locations that correspond approximately to those used in the calculations. There is good agreement between the observed and calculated waveforms.

### B. Edge Compensation with External Electrodes

The non-uniform weighting potential of the simple grid electrode structure can be thought of as being due to the greater local influence of the grid electrode closer to a particular edge of the detector. One method to compensate for this is by adding an external electrode on each side of the detector connected to the other grid electrode as shown in Fig. 11. By adjusting the size and location of these external electrodes, a much more uniform weighting potential can be obtained, as shown in Fig. 12. The weighting potential contours in the bulk of the detector are no longer tilted indicating good uniformity. This improvement is reflected in the calculated induced charge signals (Fig. 13). The induced charges on the two grids are nearly identical when the drifting charge is away from the gridded surface, independent of the position of the charge creation. Figure 14 shows the measured induced signals when the external electrodes are added to the detector.

### C. Edge Compensation with a Modified Grid Pattern

Another method to compensate for the edge effect is to modify the grid electrode pattern on the detector. The design used in this investigation is shown in Fig. 15. The width of the grid line next to the one closest to the edge is increased to counterbalance the dominance of the edge grid line. Figures 16 and 17 show respectively the calculated weighting potential

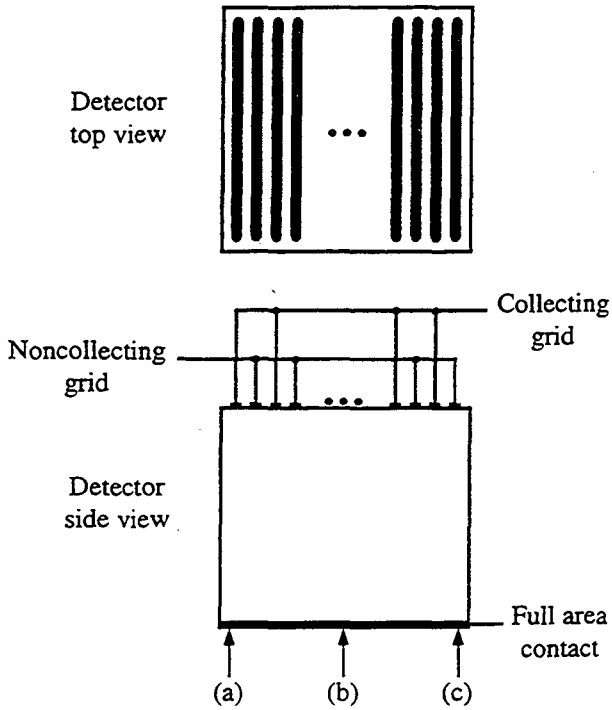


Figure 7. Schematic diagram of the simple coplanar-grid detector. The detector has an area of $9.6 \times 9.6$ mm$^2$ and a thickness of 8.5 mm. There are 18 grid electrodes of 0.25 mm width and 0.5 mm pitch.

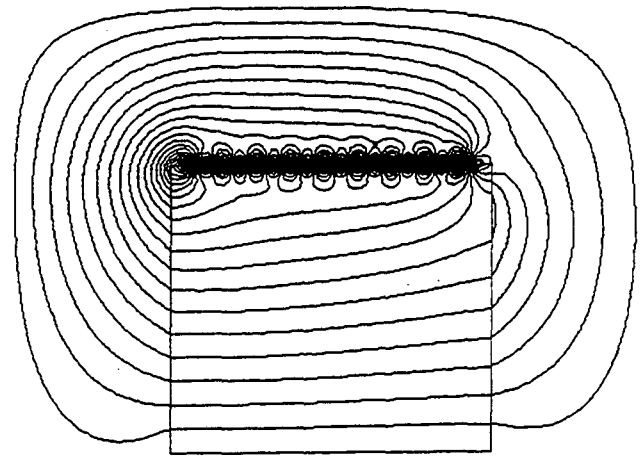

Figure 8. Calculated equipotential contour plot of the collecting grid weighting potential for the simple coplanar-grid detector of Fig. 7.

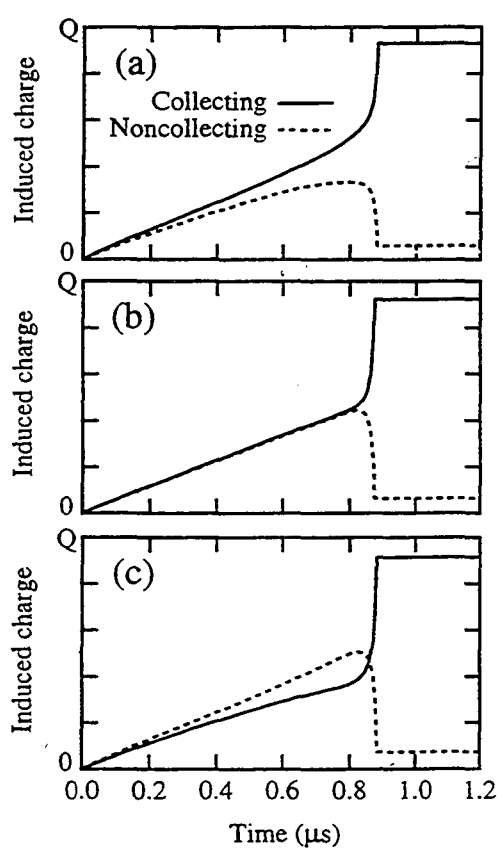


Figure 9. Calculated induced charge pulses on the grid electrodes of the simple coplanar-grid detector of Fig. 7 due to a charge $Q$ originating near the full area contact at each of the three positions indicated in Fig. 7.

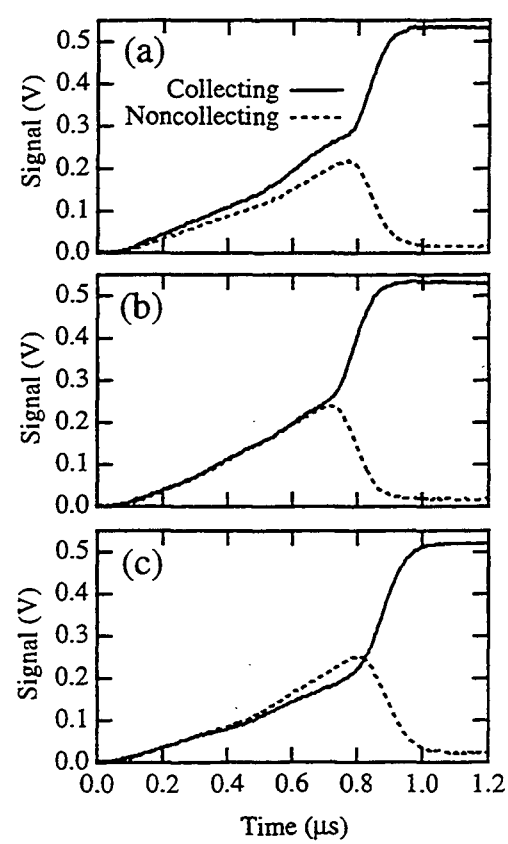


Figure 10. Measured induced charge pulses on the grid electrodes of the simple coplanar-grid detector of Fig. 7 generated by placing a collimated alpha particle source at each of the three positions indicated in Fig. 7.

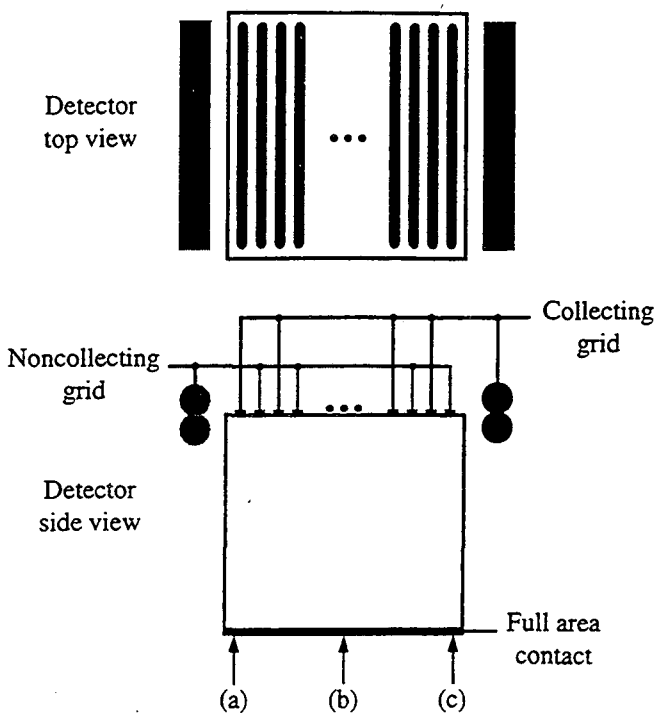


Figure 11. Schematic diagram of a simple coplanar-grid detector identical to that of Fig. 7 except with the addition of external wires for edge effect compensation.

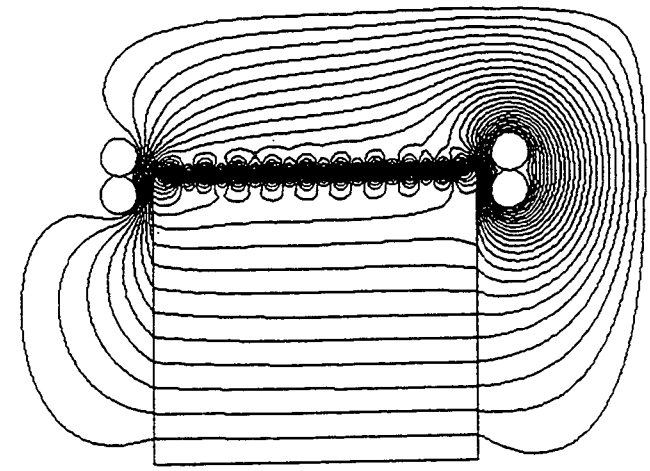

Figure 12. Calculated equipotential contour plot of the collecting grid weighting potential for the externally compensated detector of Fig. 11.

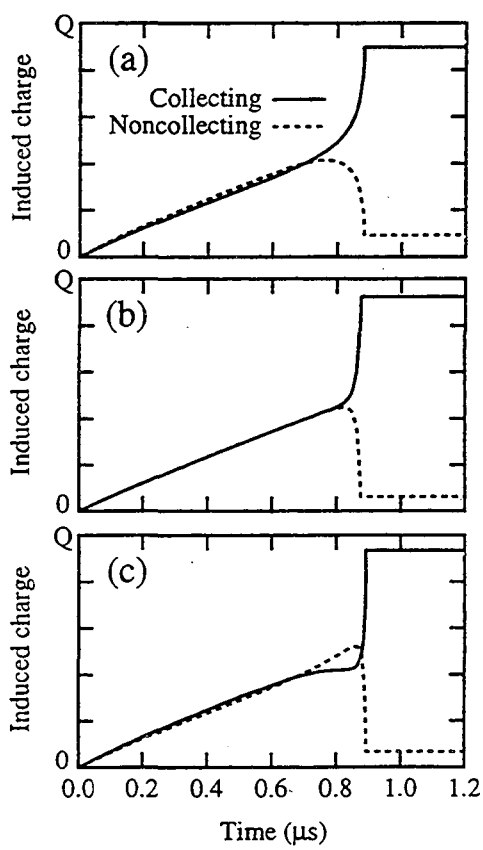


Figure 13. Calculated induced charge pulses on the grid electrodes of the externally compensated detector of Fig. 11 due to a charge $Q$ originating near the full area contact at each of the three positions indicated in Fig. 11.

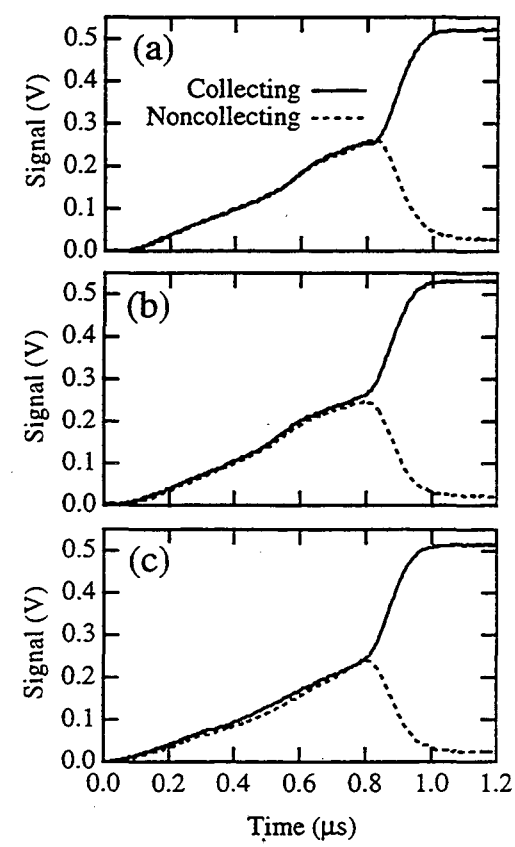


Figure 14. Measured induced charge pulses on the grid electrodes of the externally compensated detector of Fig. 11 generated by placing a collimated alpha particle source at each of the three positions indicated in Fig. 11.

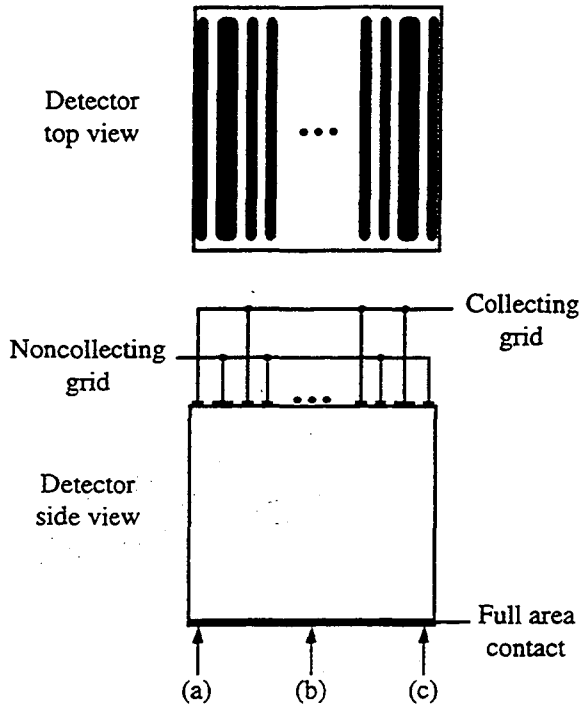


Figure 15. Schematic diagram of a coplanar-grid detector in which the grid pattern has been modified in order to correct for edge effects. The modification consists of widening the two grid lines next to the edge grid lines

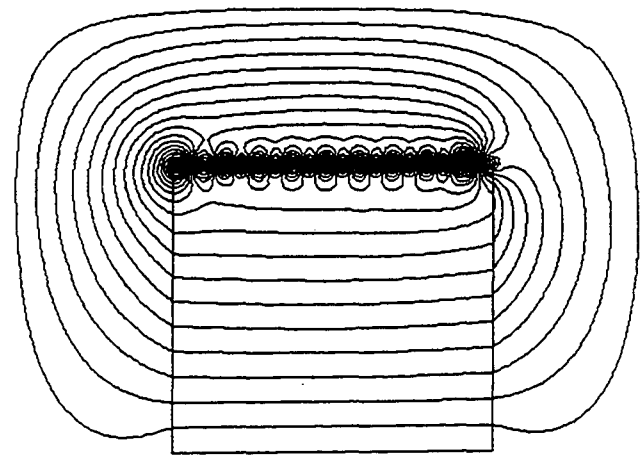

Figure 16. Calculated equipotential contour plot of the collecting grid weighting potential for the modified grid pattern detector of Fig. 15.

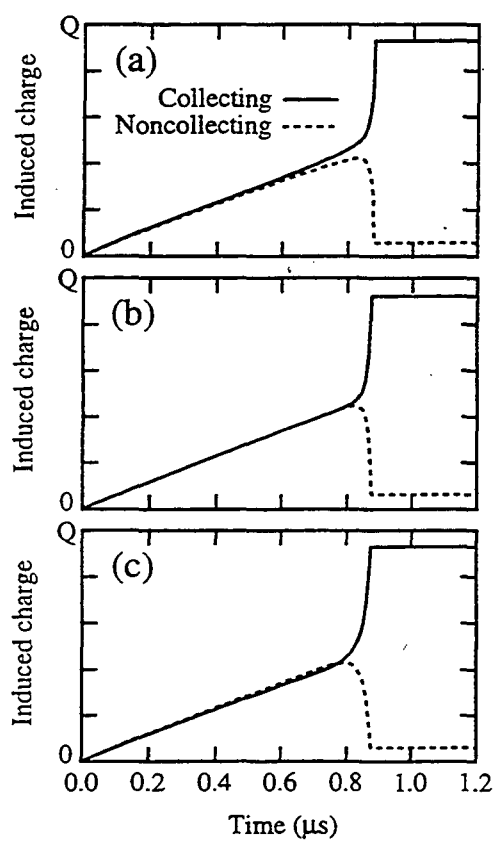


Figure 17. Calculated induced charge pulses on the grid electrodes of the modified grid pattern detector of Fig. 15 due to a charge $Q$ originating near the full area contact at each of the three positions indicated in Fig. 15.

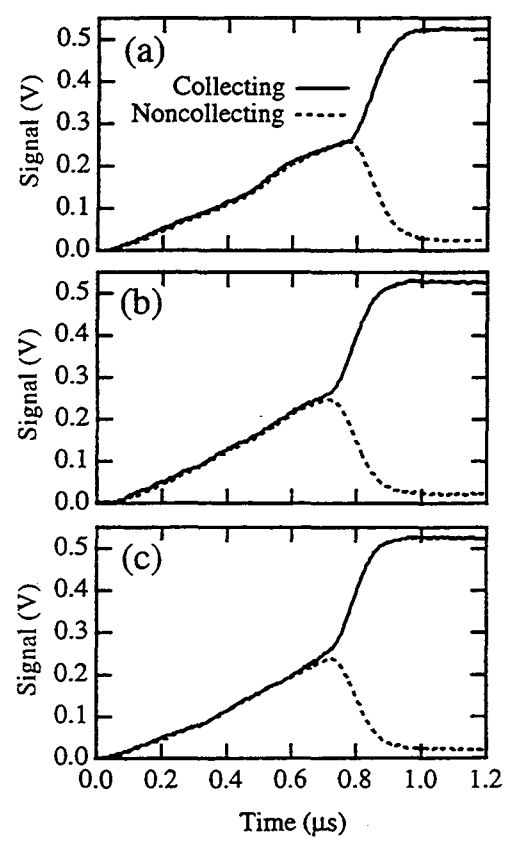


Figure 18. Measured induced charge pulses on the grid electrodes of the modified grid pattern detector of Fig. 15 generated by placing a collimated alpha particle source at each of the three positions indicated in Fig. 15.

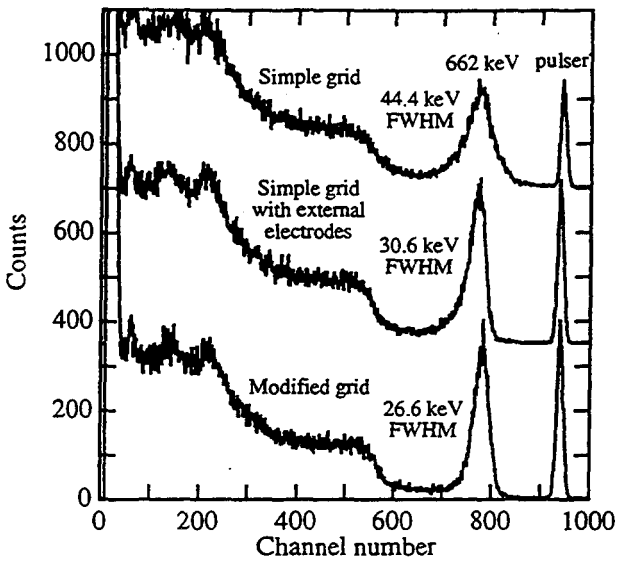


Figure 19. Measured spectra of $^{137}Cs$ obtained with the same CdZnTe crystal in each of the three detector configurations described in Figs. 7, 11, and 15.

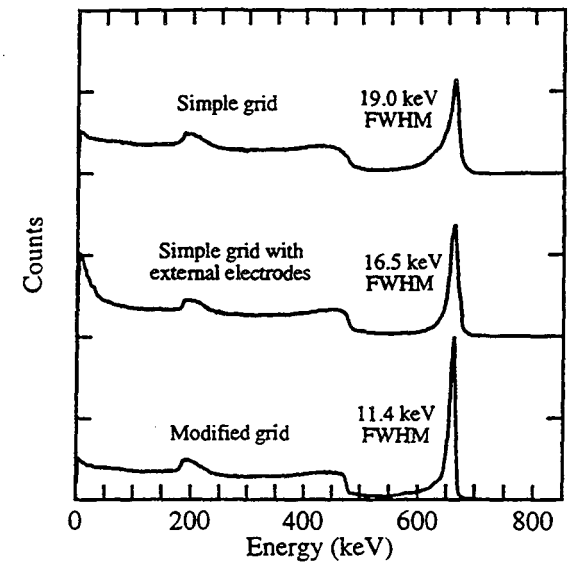


Figure 20. Calculated spectra of $^{137}Cs$ obtained assuming the three detector configurations described in Figs. 7, 11, and 15.

and signal response. The measured signal response is shown in Fig. 18. Again, a substantial improvement in uniformity is obtained, as compared to the simple grid pattern.

### *D. Spectral Performance*

Figure 19 compares the $^{137}Cs$ spectra measured with each of the three detector configurations. The relative gain $G$ of the two grid signals was optimized to give the best energy resolution in each case. From this figure it is clear that the improved uniformity in the detector weighting potentials of the edge-compensated detectors has lead to a significantly better energy resolution. This demonstrates the importance of edge effects and the substantial improvements that can be achieved by simple modifications of the electrode configuration. Simulated pulse-height spectra for the three grid designs are shown in Fig. 20. Electronic noise is not included in the simulation. Results of the calculation show qualitative agreement with experiment. Namely, the compensated detectors produce significantly improved spectral response. The large improvements in the FWTM and in the peak-to-Compton ratio for the compensated designs indicate a significant reduction in tailing. The measured energy resolution in all cases is significantly worse than that from the modeling even with the electronic noise contributions subtracted. We attributed this to non-uniform charge transport properties of the CdZnTe material used in the experiment.

## V. CONCLUSIONS

We have shown that edge effects in coplanar grid detectors can significantly affect energy resolution. Such effects however can be compensated quite effectively by using external electrodes or by modifying the grid electrode structure on the detector. Alpha particle scanning provides an effective method for characterizing the charge induction characteristics of the detector and is therefore useful for evaluating electrode designs. The computer model was able to predict the induced charge signals and the improvements in spectral performance for the edge compensated detector designs, and is therefore shown to be a useful tool for future detector development.

## VI. ACKNOWLEDGMENTS

This work was supported by the DOD Office of Special Technology, Technical Support Working Group (TSWG), Project Number T-135. The detector modeling effort is supported by the U.S. Department of Energy, Office of Nonproliferation and National Security.

## VII. REFERENCES

[1] E. Sakai, "Present Status of Room Temperature Semiconductor Detectors," *Nucl. Instr. Meth.*, vol. 196, no. 1, pp. 121-130, May 1982.

[2] J. F. Butler, C. L. Lingren and F. P. Doty, "$Cd_{1-x}Zn_xTe$ Gamma Ray Detectors," *IEEE Trans. Nucl. Sci.*, vol. 39, no. 4, pp. 605-609, Aug. 1992.

[3] P. N. Luke, "Unipolar Charge Sensing with Coplanar Electrodes - Application to Semiconductor Detectors," *IEEE Trans. Nucl. Sci.*, vol. 42, no. 4, pp. 207-213, Aug. 1995.

[4] P. N. Luke and E. E. Eissler, "Performance of CdZnTe Coplanar-Grid Gamma-Ray Detectors," *IEEE Trans. Nucl. Sci.*, vol. 43, no. 3, pp. 1481-1486, June 1996.

[5] T. Prettyman, C. Cooper, P. Luke, *et al.*, "Calculation of the Response of Semiconductor Detectors," *J. Appl. Rad. Isot.*, (to be published).

[6] T. Prettyman, T. Reilly, M. Miller, *et al.*, "Advances in Nuclear Instrumentation for Safeguards," Proceedings of the Joint ESARDA-INMM Workshop "Science and Modern Technology for Safeguards" Arona, Italy, 28-31 October, 1996.

[7] S. Ramo, "Currents Induced by Electron Motion," *Proceedings of the I.R.E.*, vol. 27, pp. 584-585, Sept. 1939.

ERNEST ORLANDO LAWRENCE BERKELEY NATIONAL LABORATORY
ONE CYCLOTRON ROAD | BERKELEY, CALIFORNIA 94720

Prepared for the U.S. Department of Energy under Contract No. DE-AC03-76SF00098